

Synthesis and Characterization of Composite Materials HDPE/HA and PMMA/HA Prepared by Sonochemistry

C. Parra,^{1,2} G. González,^{2,4} C. Albano^{*3,5}

Summary: In the present work, the synthesis and characterization of composite materials based on HDPE, and PMMA with nanometric hydroxyapatite, are studied. Composites preparation was carried out by dilutions of the commercial polymers, using decaline as solvent for the polyolefin and 2-butanone for PMMA. In the synthesis of Hydroxyapatite (HA), ammonium phosphate $[(\text{NH}_4)_2\text{HPO}_4]$ and calcium hydroxide $[\text{Ca}(\text{OH})_2]$ were used as precursors. Composites with 20, 30 and 40 wt% of HA were prepared. The polymer dilutions and the precursors of the HA were placed simultaneously in a reactor under ultrasonic radiation at 20 kHz, for periods of 15, 25 and 35 min. The products obtained were characterized by FTIR, TGA, TEM, XRD and biocompatibility studies were also carried out. The results showed the presence of nanometric HA and clear interactions between HA and PMMA polymers were observed by FTIR. These results were corroborated by TEM showing that nanometric HA particles are encapsulated into the polymeric PMMA matrix. For the composites of HDPE, these interactions were not observed.

Keywords: biocompatibility; composites; HDPE; hydroxyapatite; PMMA; ultrasonic radiation

Introduction

In the last years, composites made of polymers and ceramics fillers represent a new class of materials of high interest. Polyolefins usually show low toxicity and has been recommended as a suitable material for bone tissue substitution.^[1,2] On the other hand, hydroxyapatite is a biocompatible ceramic that is present in natural bones, consequently, composite materials based on polyolefins filled with HA have been studied by some authors for applications

as biomaterials.^[3,4] They concluded that these materials showed suitable hardness and rigidity, as well as high biocompatibility for tissue replacement.

Poly (methyl methacrylate) (PMMA) is one of the popular bone repairing materials for bone fixation joints.^[5,6] The addition of hydroxyapatite(HA), offers the possibility of improving strengthening. HA can add bioactivity to the composite materials and the extent of this activity is dependent of the volume fraction of HA incorporated.

The interfacial adhesion and the adequate dispersion of HA in the polymer matrix are one the important factors governing the mechanical behavior of these composites.^[7,8] The control of the interfacial interactions is a difficult task; one of the methods employed is the use of coupling agents. Sousa *et al.*^[7] studied HDPE-HA composites containing zirconate and titanate coupling agents, however, these additives may have detrimental effects on the biocompatibility properties of the material.

¹ Instituto Universitario de Tecnología “Dr. Federico Rivero Palacio”, Departamento de Química, Venezuela

² Lab. Ciencia e Ing. de Materiales, Dpto. Ing.; IVIC. Apdo. 21827, Caracas 1020-A, Venezuela

³ Laboratorio de Polímeros, Centro de Química. IVIC. Apdo. 21827, Caracas 1020-A, Venezuela

⁴ Escuela de Física, Facultad de Ciencias, UCV. Caracas, Venezuela

⁵ Escuela de Ingeniería Química, Facultad de Ingeniería. UCV. Caracas, Venezuela
E-mail: calbano@ivic.ve; gemagonz@ivic.ve

The methods of synthesis for composite formation can be grouped in physical and chemical. Physical methods^[9] (extrusion, mechanical mixing, etc), in general only form weak Van Der Waals bonding that do not strongly contribute to the interface interaction. Chemical methods can form stronger bonding at the interface modifying the final properties of the composite.

One alternative method of improving the interface interaction and dispersion of the filler in the polymer matrix is the *in situ* synthesis^[10] by ultrasonic irradiation.^[11,12] This method has the advantage of avoiding toxicity due to coupling agents and therefore can potentially be used for the synthesis of materials for biomedical applications.

The objective of the present work was to synthesize composite materials (polymer / hydroxyapatite) by *in situ* synthesis using high frequency ultrasonic radiation. The polymers used were poly(methylmethacrylate) (PMMA) and high density polyethylene (HDPE).

Experimental Part

Materials

Two commercial polymers were employed, a high density polyethylene (HDPE, 2908A, density 0.9595 g/cm³), and polymethylmethacrylate (PMMA, MD-2002, density 0.9233 g/cm³), using decaline as solvent for the polyolefin and 2-butanone for PMMA (Figure 1). Hydroxyapatite was synthesized using calcium hydroxide, Ca(OH)₂, and ammonium phosphate, (NH₄)₂HPO₄ as initial reagents.

Syntheses of the Composites

Composite materials were obtained from the *in situ* synthesis of hydroxyapatite (HA)

in dissolved PMMA or HDPE, using the specific solvent according to the chemical structure of each polymer, decaline for HDPE and 2-butanone for PMMA. In the case of HDPE/HA composite, the polymer and decaline were heated up to total dissolution of the polymer, HA precursor components (calcium hydroxide and ammonium phosphate) were added in stoichiometric amounts to obtain composites with 10, 20, 30 and 40 wt% of HA. Immediately the samples underwent ultrasonic radiation for different periods (15, 25 and 35 min). An ethanol/water solution (1:1) was added to precipitate the material. The solution was kept resting for 1h and then centrifuged. To eliminate any remaining decaline the material was thoroughly washed several times in cold ethanol. Composites were dried at 90 °C and weight to determine the synthesis conversion.

PMMA/HA composites syntheses were performed by a similar procedure, but using 2-butanone as solvent. Composites were dried at 60 °C.

Characterization of the Composites

FT-IR spectra were taken from compression-molded films of the composites. These spectra were recorded in a Nicolet Magna_IR 560 E.S.P. Spectrometer after 32 scans and at 2 cm⁻¹ of resolution and a Perkin Elmer FTIR spectrum 100 equipment with a resolution of 0.5 cm⁻¹.

To determine the weight percentage of the synthesized hydroxyapatite thermogravimetric test (TGA) were carried out, using a TA Q600 equipment in nitrogen atmosphere, using a heating rate of 10 °C/min.

Transmission electron microscopy (TEM) analyses were performed using a Phillips CM10 microscope. Samples were prepared by ultramicrotomy without any further treatment.

XDR patterns were recorded using a diffractometer Siemens, Model D 500, in the 2θ range of 20°–60°.

Biological test were carried out to evaluate cellular adhesion and proliferation for the different materials. The materials were washed in ethanol to remove super-

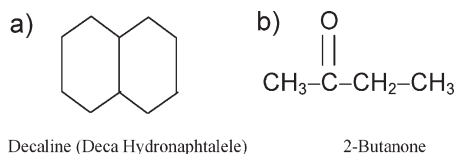


Figure 1.
Molecular structure of the solvents used.

ficial grease. Then, they were washed extensively with deionized water and finally sterilized using gamma radiation with 25 kGy dose. The adhesion capability of bone cells, derived from neonatal calvaria rats, was obtained following the procedure previously described.^[13] The effect of seric proteins contained in Fetal Bovine Serum (FBS) in bone cell adhesion on PMMA, HDPE and the composite samples was evaluated. Cell adhesion was evaluated employing the commercial kit CyQuant (Invitrogen®) with a fluorescent colorant. Experiments with and without Fetal Bovine Serum were carried out. Samples of 6 mm diameter were tested using a 96 well-plate (for tissue culture, NUNC). A 4×10^4 cells/ml suspension was seeded with the different materials and control (which corresponds to an empty well). After 16 h of incubation in optimal culture conditions (37 °C in a fully humidified atmosphere at 5% CO₂ in air), adhered cells were quantified using the CyQuant kit. Fluorescence was measured directly in a fluorimeter with filters of 485 nm excitation and 535 nm emission wavelengths. Measurements were taken after 16 h of incubation time.

Results and Discussion

Synthesis and Characterization of Hydroxyapatite

The synthesis of Hydroxyapatite was carried out in the different solvents used for each polymer (decaline and 2-butanone) under ultrasonic radiation for different periods. The results were very similar for all periods. Figure 2 shows typical FTIR spectra of these syntheses performed in each of the solvents used. The spectra correspond to hydroxyapatite structure,^[14] showing all the characteristic absorption bands, independently of the synthesis conditions. The OH stretching in the range 3400–3500 cm⁻¹ and the phosphate vibrations at 1100–1030 cm⁻¹, 960 cm⁻¹ and 570–600 cm⁻¹.

Figures 3 and 4 show the XRD patterns of HA synthesized in 2-butanone and decaline respectively, at different periods

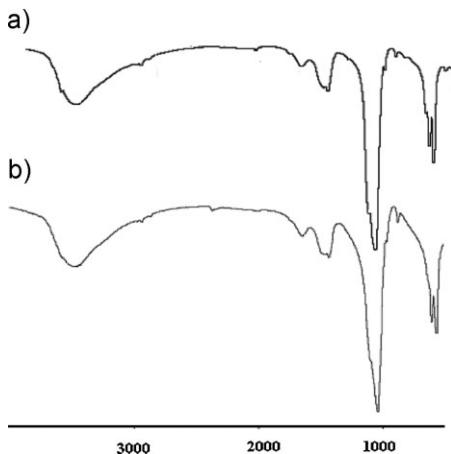
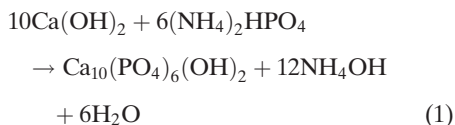


Figure 2. FTIR spectra of HA synthesized in a) 2-butanone, b) decaline.

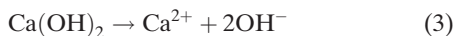
of reaction under ultrasonic radiation. The similarity of the diffractograms can be observed clearly for both conditions, indicating that the material obtained is not affected by solvent or reaction time under ultrasonic radiation, consistent with the FTIR results. The nanometric grain size, evidenced from the peak width of the diffractograms and also corroborated by TEM analysis (Figure 5), is maintained for the different synthesis conditions.

The conversion results are shown in Table 1, indicating that HA synthesis in 2-butanone yields the maximum conversion (98%) compared to decaline (40–70%). This can be due to easiness of the reactants for dissociation in ionic species in 2-butanone solvent.

The general equation for HA formation is:



and the initial reactant dissociate in ionic species:



This process has a higher velocity in 2-butanone due to solvation of the ions

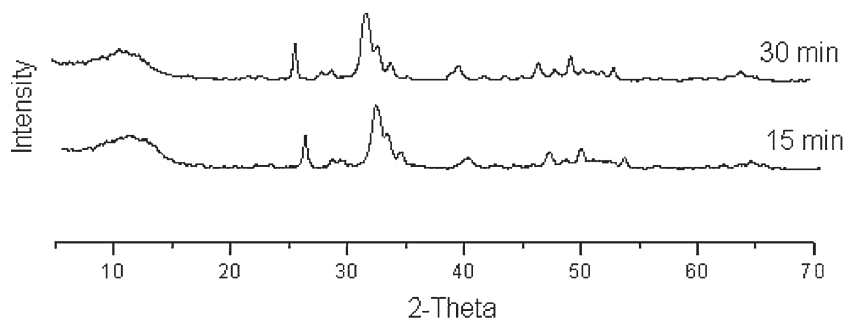


Figure 3.
XRD pattern of HA synthesized in 2-butanone.

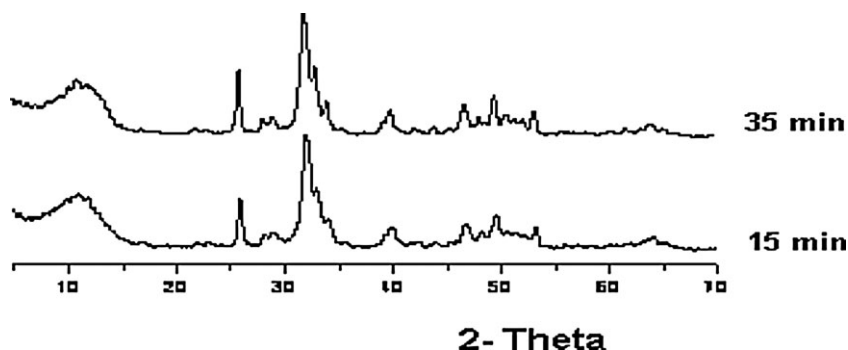


Figure 4.
XRD pattern of HA synthesized in decaline.

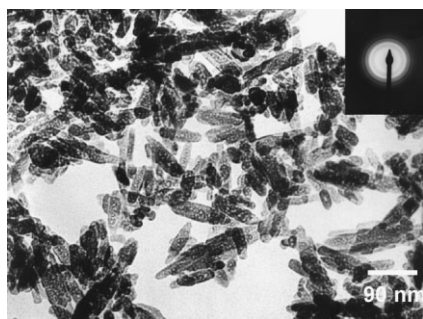


Figure 5.
TEM bright field image of HA synthesized in 2-butanone, inset electron diffraction pattern.

Table 1.
Conversion values of HA synthesized in different solvents for different ultrasonic radiation periods.

Irradiation time (min)	Conversion (%) in 2-butanone	Conversion (%) in decaline
15	93.78	40.70
30	97.07	69.15

in this solvent. Additionally, cavitation favors the reactivity of the species formed.^[15] On the other hand, decaline is a non polar solvent and the reactions occur due to formation of the ionic species by the ultrasonic waves. Therefore, this process is slower, the solvent has higher viscosity and cavitations are confined to a closer region near the wave probe.

Synthesis and Characterization of Composites Polymer/Hydroxyapatite

Figures 6 and 7 show some of the FTIR spectra obtained for the different composites as-synthesized and after calcination. Figure 6 shows the spectrum of the synthesis obtained after ultrasonic irradiation for 25 min, of PMMA and HA precursors to give a theoretical percentage of 20 wt.%. The spectrum shows overlapping vibration bands of PMMA and HA. The PMMA bands are in the region 3000–2852 cm^{-1} , 1737 cm^{-1} , 1440–1157 cm^{-1} and

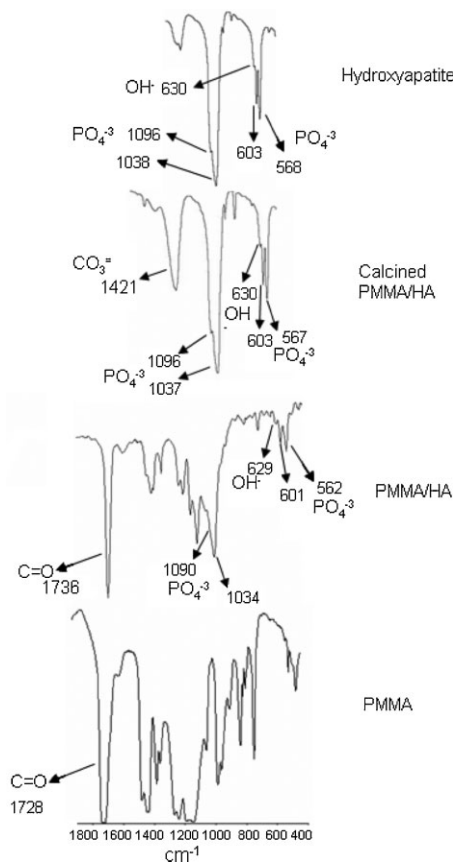


Figure 6.

FTIR of composite PMMA/HA, comparison with spectra of calcined material and pure HA and PMMA spectra.

1000–800 cm^{-1} . HA bands are in the regions: 1100–1030 cm^{-1} , 960 cm^{-1} and 570–600 cm^{-1} . The spectrum of the sample after calcination shows all the bands corresponding to HA. A slight shifting of 4 cm^{-1} is observed in the phosphate bands at 1087–1040 cm^{-1} with respect to pure synthesized HA, and also a shifting of 8 cm^{-1} in the carbonyl groups of the composite PMMA/HA with respect to pure PMMA. This suggests an interaction between the polymer matrix and HA.

Figure 7 shows the FTIR spectrum of the material synthesized with HDPE and HA precursors under ultrasonic irradiation for 35 min, to give a theoretical HA percentage of 20 wt.%. The composite shows the characteristic HDPE bands observed at

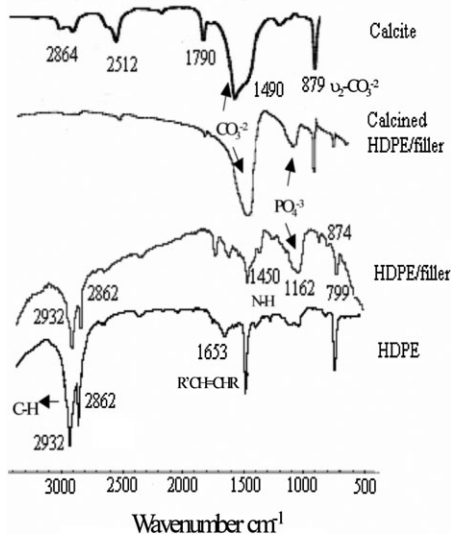


Figure 7.

FTIR spectra of composite HDPE/filler, comparison with spectra of calcined material and pure calcite and HDPE spectra.

2932 and 2862 cm^{-1} corresponding to C–H bonding of the CH_2 groups. Also, vibration bands in 3350 and 1450 cm^{-1} are observed that can be assigned to N–H bond of an ammonium compound^[16] and vibration bands in the region 1162 and 1043 cm^{-1} associated to phosphate groups. The FTIR spectrum of the calcined sample shows the vibration bands associated to phosphate groups in 1162 and 1043 cm^{-1} , and the vibration band around 1490 cm^{-1} associated to carbonate groups. Also, vibration bands in 799 and 874 cm^{-1} corresponding to calcite [CaCO_3] that was formed during the synthesis process.

This implies that HA was not formed in this synthesis, probable due to high viscosity of the media (HDPE chains swollen in decaline) restricting diffusion and transport of ionic species, therefore impeding HA formation. On the other hand, shifting of vibration bands was not clearly observed, implying that there is no interaction between the polymer and the filler.

Figures 8 and 9 show the XRD patterns of the synthesized composites. The evolution of phase formation with ultrasonic

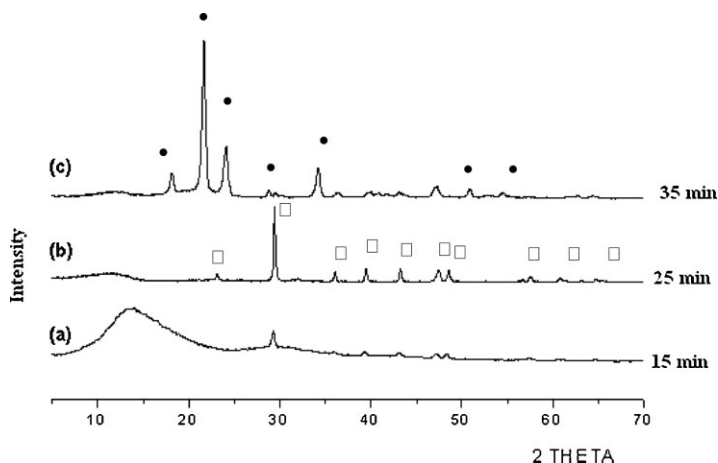


Figure 8.

XRD patterns of HDPE/filler composite: ● polyethylene, □ calcite.

radiation time is shown for the composite HDPE/filler. The formation of calcite is progressively observed for radiation time (15 and 25 min). After 35 min of ultrasonic radiation crystalline HDPE is clearly observed together with calcite. The crystallization of HDPE for long radiation periods could be explained based in observations of other experiments^[17] of composites HDPE/HA, prepared in solution of decaline and further irradiated in solid state with γ -rays, that resulted in a decrease in viscosity implying a decrease in molecular weight. In the present work, ultrasonic radiation for long periods induces some HDPE chains incision reactions that during cooling reorganize and crystallize, however, this does not have a marked effect on the average viscosity of the media. On the other hand, the FTIR of the composite material

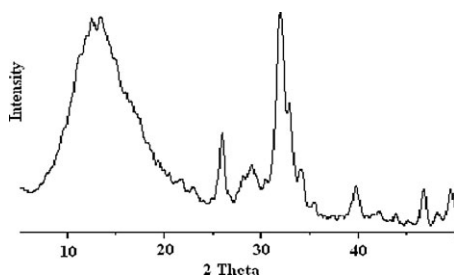


Figure 9.

XRD pattern PMMA/HA composite.

(Figure 7) showed formation of ammonium and phosphate groups that are not seen in the XRD pattern; therefore, probably an amorphous ammonium phosphate compound could also be present in this material.

Figure 9 shows the formation of HA in the amorphous PMMA matrix, all the reflections correspond to HA structure. The peak broadening implies nanometric crystal size.

Figures 10 and 11 show typical thermograms of the composites. The TGA analysis was used to determine the percentage of the inorganic phase formed in the PMMA or HDPE matrix, respectively, and also to confirm the conversion values obtained by calcination (Tables 2 and 3). In general a good correspondence exists between both techniques (TGA and calcination). DSC analysis showed that the melting point for HDPE, in the composite, was 137 °C, and the glass transition temperature of PMMA, in the composite, was 128 °C. These results are in good agreement with those reported in the literature,^[18] implying that the filler does not strongly affect the thermal properties of both polymers.

Table 2 shows the conversion percentage of the *in situ* synthesis of the composites PMMA and HDPE. The values presented for HDPE are lower than the theoretical conversion (40–50%) calculated based on

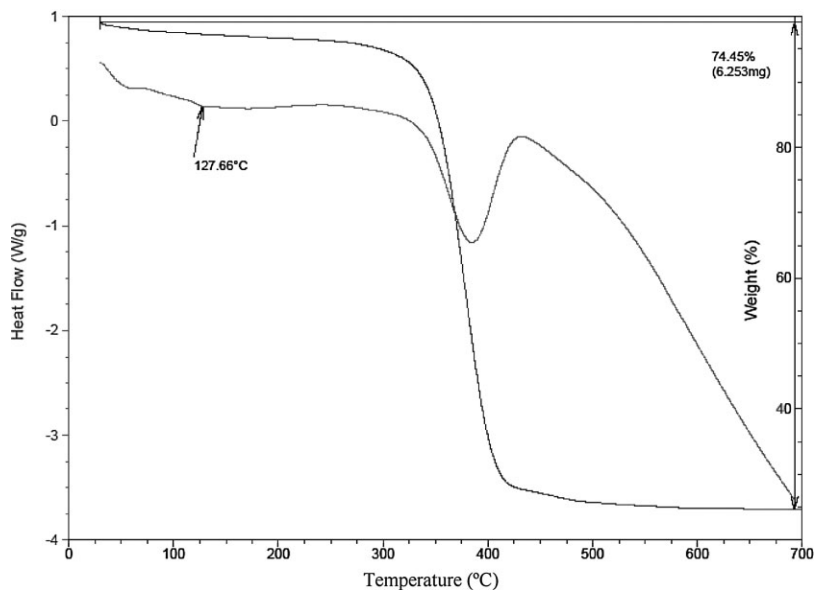


Figure 10.

TGA and DSC of PMMA/HA (30%) 25 min of ultrasonic irradiation.

the precursors addition to obtain HA. The composites PMMA/HA show a good approximation to the theoretical values. This behaviour is attributed to the polarity characteristics of this polymer and the

degree of miscibility of HA in the dissolved PMMA in 2-butane. From the FTIR spectra interactions between the ester group of PMMA and the phosphates groups of HA were evident.

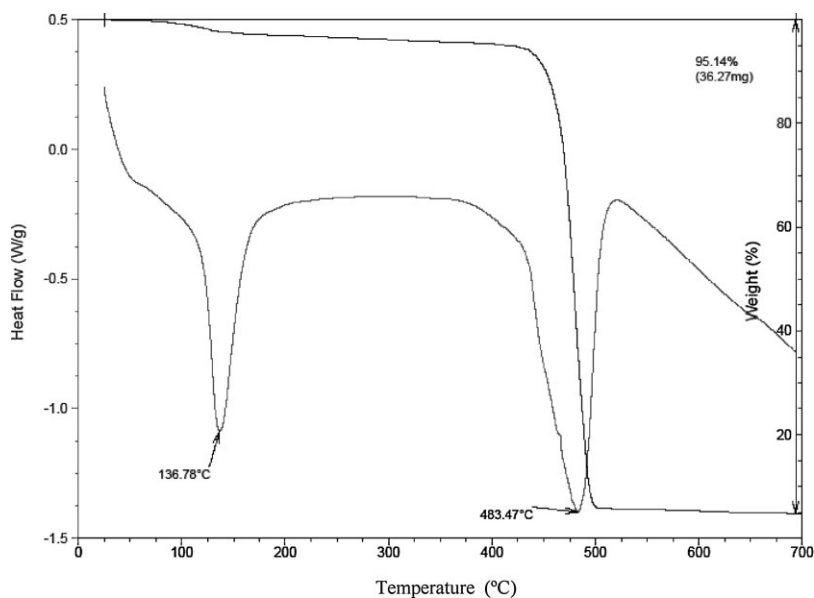


Figure 11.

TGA and DSC of HDPE/filler composite 25 min of ultrasonic irradiation.

Table 2.

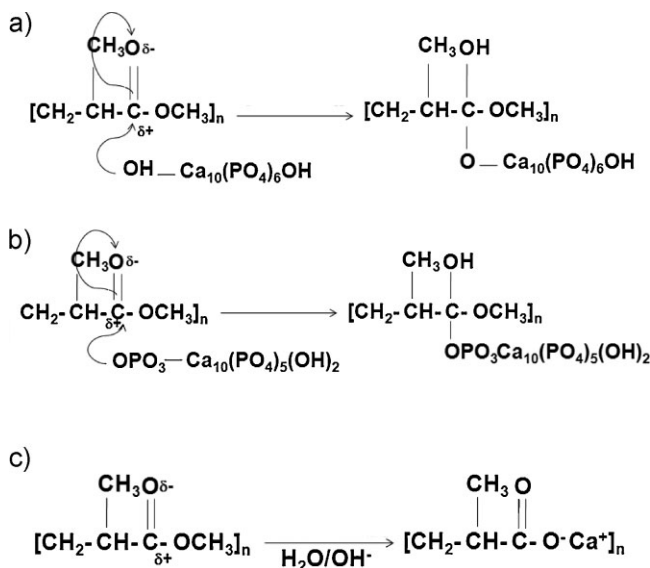
Conversion of HA obtained by “in situ” synthesis in PMMA and HDPE.

Reaction time (min)	Theoretical conversion (%)	Experimental Conversion in PMMA (%)	Experimental Conversion in HDPE (%)
15	10	7.18	4.08
25		6.39	4.87
35		6.50	3.67
15	20	5.67	6.43
25		6.19	7.74
35		6.75	7.56
15	30	29.90	15.51
25		25.50	16.14
35		28.41	15.95
15	40	39.07	20.99
25		36.08	19.87
35		39.14	18.60

Three possible mechanisms of these interactions are proposed in Figure 12: a) the Ca^{+2} ions of HA form a bond with the COOCH_3 groups of PMMA, b) the negative ions of HA (PO_4^{-3}) are susceptible of reacting with the carbonyl group by a nucleophilic attack^[19] and c) the substitution of the methoxy group of the ester of PMMA by the Ca^+ ion is responsible of the shifting observed in the carbonyl group. This can be a consequence of the basic media generated by the ammonium hydroxide (Eq. 1).

Figure 13 shows the morphology of the composite HDPE/filler by TEM, electron dense zones associated to agglomerates of the inorganic compound disperse in the polymer matrix can be observed. In Figure 13b a magnified region showing crystals with hexagonal morphology, identified as calcite from the electron diffraction pattern (inset).

Figure 14 shows a TEM image of PMMA/HA composite, hydroxyapatite particles encapsulated in a thin film of PMMA, forming “pockets” of the

**Figure 12.**

Proposed mechanism of PMMA/HA interactions.

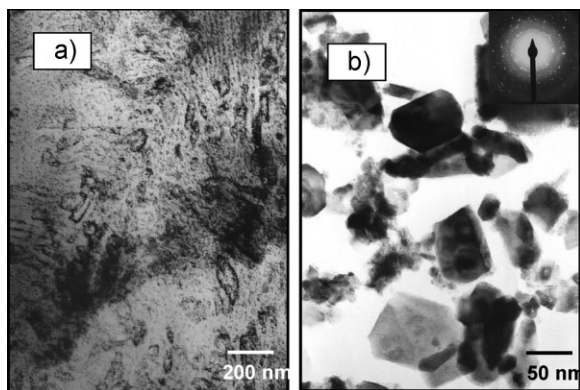


Figure 13.
TEM bright field images of HDPE/filler composite a. general view, b. magnified image.

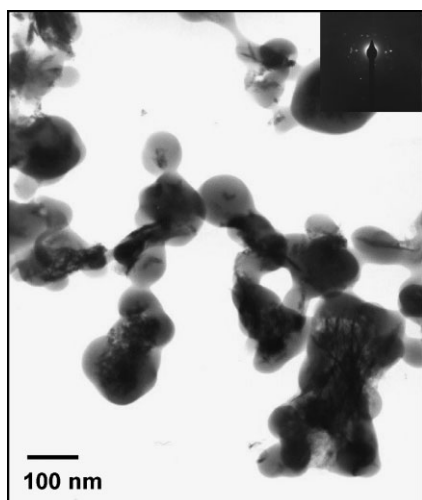


Figure 14.
TEM bright field image of PMMA/HA composites.

composite material, can be observed. As mentioned above (FTIR analysis) polymer/HA interactions were formed during the synthesis process. Also a good dispersion of HA due to the ultrasonic process is obtained.

Biological Tests

Figure 15 shows the cellular adhesion results after 16 h of culture with and without SBF (bovine fetal solution) as culture media for the polymers and the composite materials.

It can be observed that the cellular adhesion of the composites is higher than for the pure polymers or the control sample. The composites PMMA/HA show the highest cellular adhesion results even without the presence of SBF, suggesting that the interactions formed between the functional polar groups of the polymer and HA are

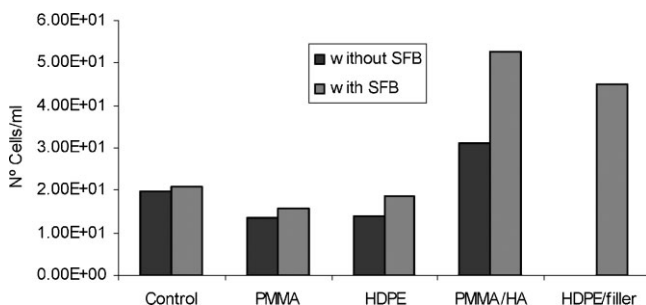


Figure 15.
Cell adhesion test of PMMA and HDPE and their composites.

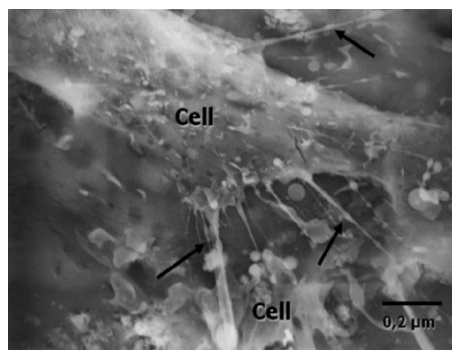


Figure 16.

SEM Image of an osteoblast on PMMA/HA composite.

responsible of the cellular adhesion and proliferation on the composite. Figure 16 is an image of an osteoblast on PMMA/HA composite, showing the cell attachment to the material through extending filopodia, indicating the biocompatibility of this surface.

For the composite HDPE/filler the cellular adhesion is slightly lower than for PMMA/HA, but much higher than for the HDPE alone, indicating that the inorganic phases formed are also biocompatible. These results suggest that this composite could also be a potential candidate for applications as biomaterial.

Conclusion

The synthesis of HA is obtained in both solvents 2-butanone and decaline. However, the conversion percentage is higher in 2-butanone.

The formation of HA in the composite material was obtained when PMMA was used, with interaction at the interface Polymer/HA. When HDPE was used a mixture of phases was obtained due to the high viscosity of the reaction media and not interaction at the interface was observed.

TEM showed HA particles encapsulated in pockets of PMMA film.

A good dispersion of the filler was observed for both polymers.

From the biological studies it can be concluded that both composites showed good cellular adhesion, although slightly better for PMMA/HA.

- [1] S. N. Nazhat, R. Joseph, M. Wang, R. Smith, K. E. Tanner, W. Bonfield, *J. Mater. Sci: Mat in Med.* **2000**, 11, 621.
- [2] K. E. Tanner, R. Downes, W. Bonfield, *British Ceramics Transactions* **1994**, 93, 104.
- [3] M. Wang, D. Porter, W. Bonfield, *British Ceramics Transactions* **1994**, 93, 91.
- [4] L. Di Silvio, *J. Mater. Sci. Mat. in Med.* **1998**, 3, 845.
- [5] M. J. Dalby, L. Di Silvio, E. J. Harper, W. Bonfield, *J. Mater. Sci. Mater. in Med.* **1999**, 10, 793.
- [6] C. Ohsuki, T. Miyasaki, M. Kyomoto, M. Tanihara, A. Osaka, *J. Mater. Sci. Mater. In Med.* **2001**, 12, 895.
- [7] R. A. Sousa, R. L. Reis, A. M. Cunha, M. J. Bevis, *J. Appl. Polym. Sci.* **2002**, 86, 2873.
- [8] C. Albano, A. Karam, G. González, N. Domínguez, Y. Sánchez, F. Manzo, C. Guzmán, J. González, M. Ichazo, P. Joskowicz, *ANTEC 2004 Proceedings*, Chicago, USA, **2004**, 3371.
- [9] M. Alexander, E. Martin, P. Dubois, M. García-Martí, R. Jerome, *Chemical Materials* **2001**, 13, 236.
- [10] D. G. Hawthorne, J. H. Hodgkin, B. C. Loft, D. H. Solomon, *J. Macromol. Sci-Chem.* **1974**, A8, 3, 649.
- [11] K. Suslick, G. Price, *Annul. Rev. Mater. Sci.* **1999**, 29, 295.
- [12] T. Mason, "Sonochemistry", Oxford University Press, New York 1999, 1–42.
- [13] K. Noris Suarez, I. Barrios de Arena, M. Vasquez, Y. Baron, Y. I. Atias, J. Bermudez, C. Morillo, Y. Olivares, J. Lira, *Rev. Latin. Am. Metal. Mater.* **2003**, 23, 82.
- [14] R. Edward, "Nondestructive Characterization of Materials X", Proceedings of the 10th International Symposium on Nondestructive Characterization of Materials, Karuizawa Japon, **2000**.
- [15] D. Walsh, T. Furuzono, J. Tanaka, *Biomaterials* **2001**, 22, 1205.
- [16] Base de datos JCPDS del Centro Internacional de data de Difracción (ICDD).
- [17] C. Albano, A. Karam, R. Perera, G. González, N. Domínguez, J. González, Y. Sánchez, *NIMB* **2006**, 247, 331.
- [18] J. Bandrup, E. H. Immergut, "Polymer Handbook", ACS, New York **1975**.
- [19] Z. Yi, L. Yubao, L. Jidong, Z. Xiang, L. Hongbing, W. Yuanyuan, Y. Weiho, *Materials Science and Engineering A* **2007**, 452–453, 512.